AJNR Am J Neuroradiol 22:1566–1569, September 2001

Case Report

Oculomotor Nerve Teratoma

Kevin R. Moore

Summary: The case of a rare, mature teratoma of the oculomotor nerve manifesting as an interpeduncular cistern mass is presented. A basilar tip aneurysm initially was suspected on the basis of lesion location and MR imaging appearance. Subsequent CT and catheter angiography studies were atypical for aneurysm, leading to surgical biopsy. Pathologic analysis revealed a well-circumscribed mass composed of mature representatives of all three major cell lines characteristic of mature teratoma. The imaging findings are described, and a brief literature review is provided.

The most common primary tumor of cranial nerves is schwannoma, although occasionally more unusual lesions are encountered. Accurate preoperative imaging diagnosis of intracranial lesions might prevent unnecessary surgical exploration and operative morbidity. In cases of diagnostic uncertainty, use of multiple imaging modalities might be most effective for elucidating the correct diagnosis. A case of a mature oculomotor nerve teratoma manifesting as a cisternal mass lesion that mimicked a basilar tip aneurysm is reported. To the author's knowledge, such a lesion has not been reported previously.

Case Report

A 54-year-old woman presented with light-headedness, headache, nonvertiginous dizziness, and gait problems, which were progressive over a 4-month period. A similar episode 2 years previously resolved spontaneously. Her medical history was noteworthy for long-standing bipolar disease, which was well controlled with carbamazepine, and anisocoria without diplopia, which had been present for 30 years. No history of collagen-vascular disease, chronic granulomatous disorder, or phakomatosis was elicited. Physical examination revealed a fully alert and normally oriented Caucasian woman. Results of a cranial nerve examination were noteworthy only for anisocoria (left pupil larger than right) with normal extraocular movement and intact visual fields. Cerebellar testing revealed bilateral dysmetria. Her gait was abnormal, characterized by a bizarre ataxic lurch and tendency to fall to the right. The Romberg's sign was positive. Her deep tendon reflexes were asymmetrically hyperreflexic, brisker on the right than left. The findings from laboratory studies, including serum carbamazepine level (6 mg/L; normal range, 4–8 mg/L), were normal.

MR imaging revealed a 1-cm heterogeneous extraaxial mass within the interpeduncular cistern that deformed the left cerebral peduncle. On nonenhanced T1-weighted images (Fig 1A), the mass had mixed intermediate (relative to gray matter) and high signal intensity areas. The mass displayed mixed intermediate and low signal intensity on conventional spin-echo T2-weighted images (Fig 1B). Intravenous administration of gadopentetate dimeglumine produced scattered areas of mild enhancement (Fig 1C). A presumptive clinical diagnosis of a partially thrombosed basilar artery aneurysm was made on the basis of the MR imaging characteristics, location, and clinical symptoms. Subsequent digital subtraction angiography, however, did not confirm the presumptive diagnosis of aneurysm, with the mass displaying a delayed blush more typical of a vascularized soft tissue mass (Fig 2A and B). CT imaging obtained to clarify the disparity between MR imaging and angiography demonstrated areas of marked hypoattenuation (-8 HU) on the nonenhanced series (Fig 3A) characteristic of fat and heterogeneous enhancement (28–70 HU) (Fig 3B), which corresponded to the blush noted at digital subtraction angiography.

Left subtemporal craniotomy with microscopic exploration revealed a 1-cm fatty nonaneurysmal mass arising from the oculomotor nerve 1.5 cm distal to the left root entry zone. The mass was densely adherent to both the left cerebral peduncle and basilar artery. The findings of intraoperative frozen pathologic examination indicated hamartoma. Because of concern about inducing a permanent oculomotor palsy, a complete resection was not attempted. Nevertheless, postoperatively the patient had a third nerve palsy that slowly resolved over subsequent follow-up examinations. Microscopic histopathologic examination using hematoxylin and eosin (H&E) and immunoperoxidase preparations (anti-S100, anti-desmin, anti–muscle-specific actin, and anti-neurofilament) was performed. Low-power H&E stain evaluation (Fig 4A) demonstrated dense collagen bundles admixed with fat cells, nerve filaments, and blood vessels. Higher power immunoperoxidase anti-desmin preparation (Fig 4B) revealed scattered skeletal muscle fibers interspersed within the dense collagenous tissue. The identification of mature representatives from all three tissue lines and absence of malignant features permitted a final tissue diagnosis of mature teratoma.

Discussion

The causes of third nerve palsies are myriad, and several comprehensive reviews describe diagnostic clinical and imaging approaches (1, 2). Oculomotor nerve palsies are more common in adults than children (3) and are nearly always acquired (4). In adults, neoplasms account for 18% of all isolated oculomotor palsies, with aneurysms (18%), diabetes mellitus (17%), trauma (12%), and other causes (inflammation, infection, migraines, idiopathic; 35%) completing the differential list (4).

Received February 19, 2001; accepted after revision April 16.

From the Department of Radiology, Section of Neuroradiology, University of Utah School of Medicine, Salt Lake City.

Address reprint requests to Kevin R. Moore, MD, Department of Radiology, Section of Neuroradiology, University of Utah School of Medicine, 1A71 Medical Center, 50 North Medical Drive, Salt Lake City, UT 84106.

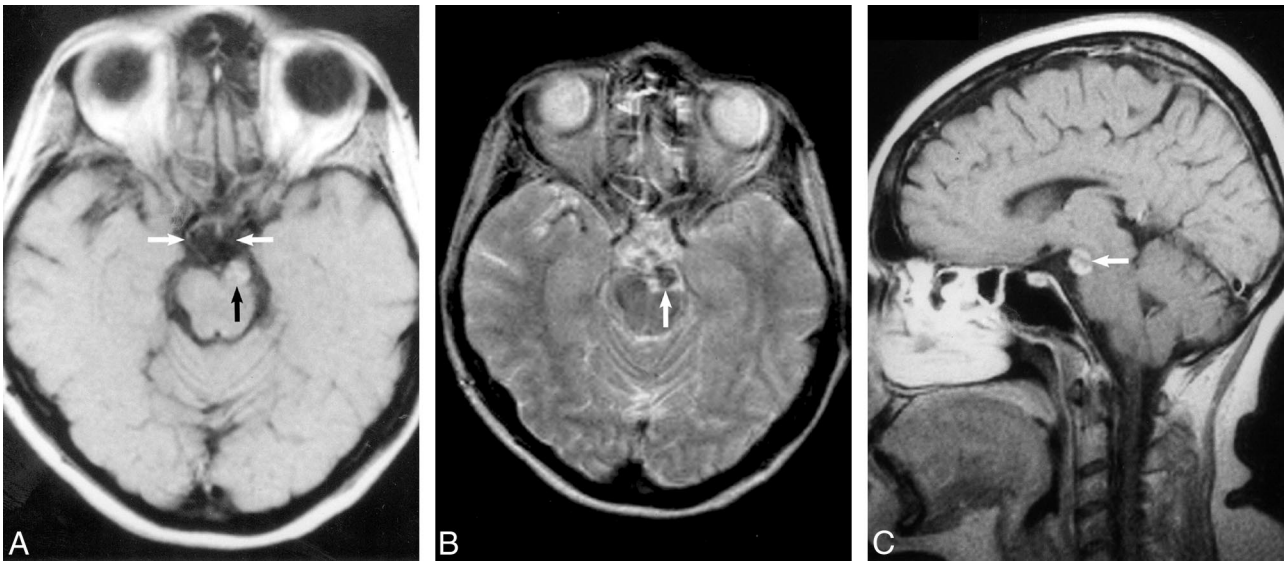

FIG 1.
A, Axial T1-weighted unenhanced spin-echo image (800/25/3 [TR/TE/excitations]) demonstrates an extraaxial mass (*black arrow*) within the interpeduncular cistern that compresses the left cerebral peduncle and displaces the left oculomotor nerve medially (*white arrows* indicate the oculomotor nerves). The mass contains heterogeneous foci of high signal intensity.
B, Conventional spin-echo axial T2-weighted image (2400/100/2) confirms a heterogeneous intermediate mass with low signal intensity (*arrow*) inseparable from the terminal basilar and left posterior cerebral arteries.
C, Sagittal enhanced T1-weighted image (550/25/4) following intravenous administration of gadopentetate dimeglumine confirms heterogeneous enhancement (*arrow*) and normal suprasellar and pineal region cisterns.

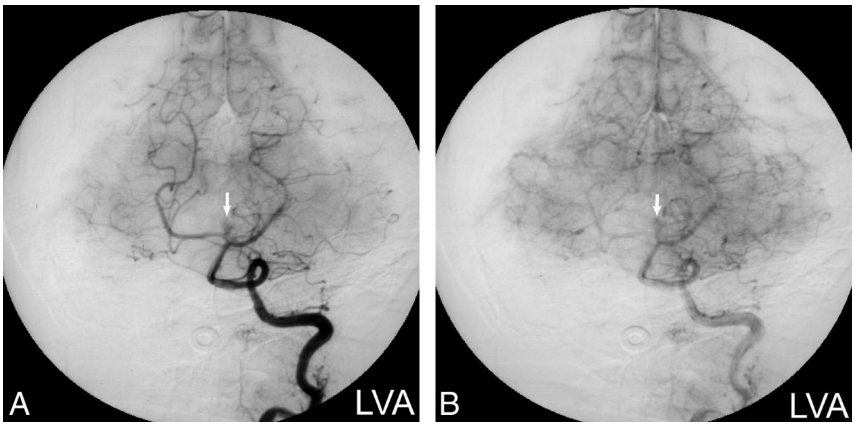

FIG 2. Digital subtraction angiograms.
A, Left vertebral artery injection (arterial phase) shows vascular enhancement of the mass (*arrow*) in a pattern atypical for aneurysm.
B, Left vertebral artery injection (capillary phase) confirms a persistent blush (*arrow*) that would be unusual for an aneurysm.

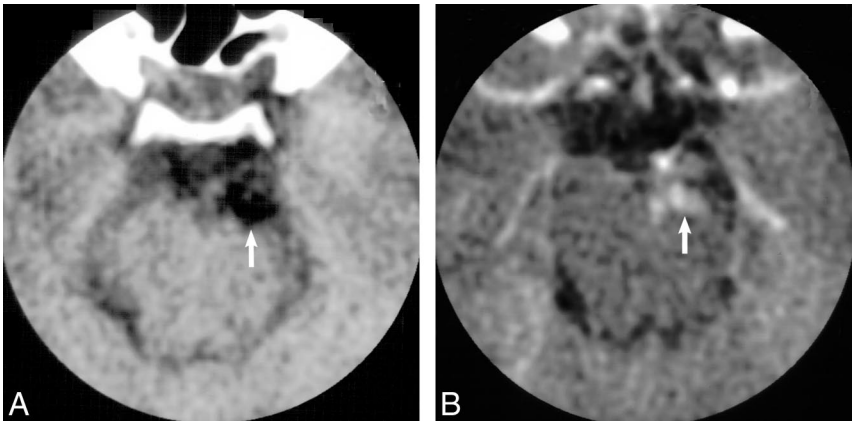

FIG 3.
A, Axial nonenhanced CT image confirms that the mass (*arrow*) is hypoattenuating (−8 HU) compared with adjacent cerebrospinal fluid (6 HU) and noncalcified.
B, Following intravenous administration of contrast material, the mass (*arrow*) reveals heterogeneous nodular enhancement (28–70 HU).

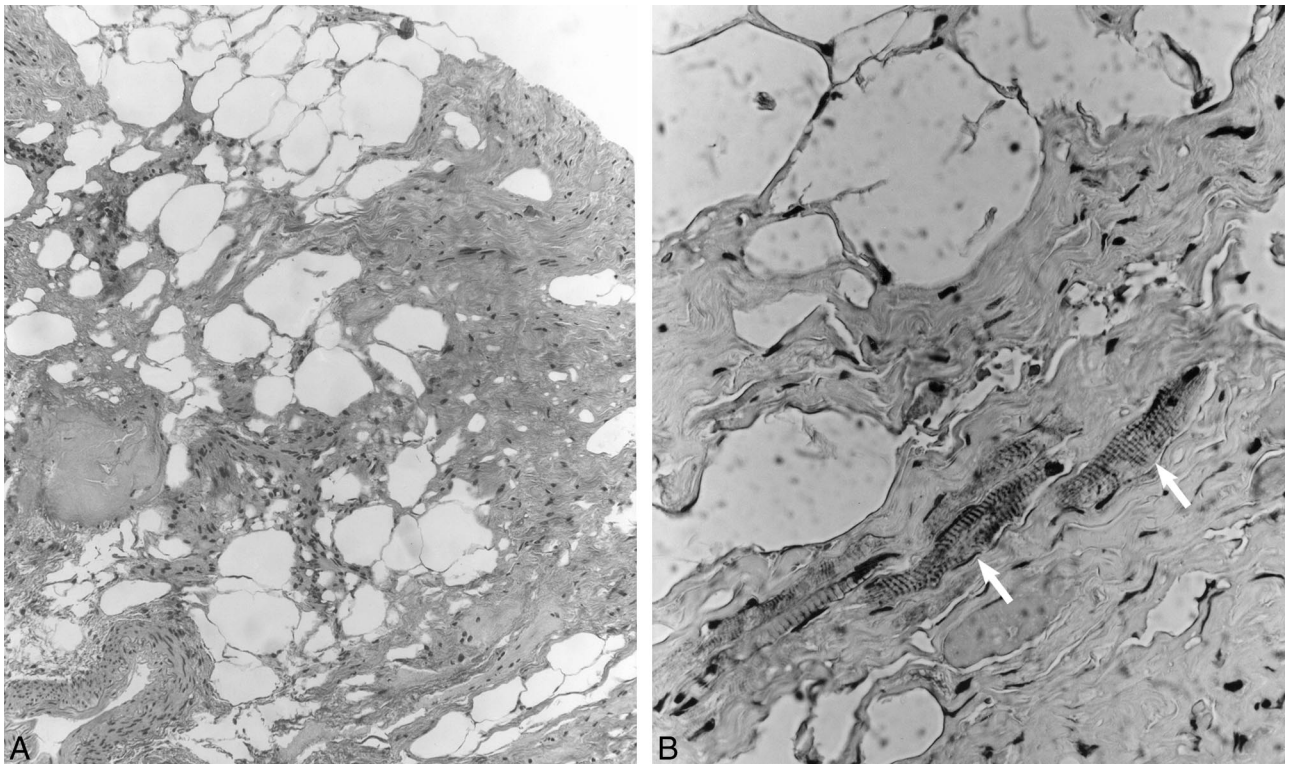

FIG 4.
A, Low-power (original magnification ×100) H&E photomicrograph demonstrates dense collagen bundles admixed with fat cells, nerve filaments, and blood vessels.
B, Higher power (original magnification ×400) immunoperoxidase (anti-desmin) preparation reveals scattered skeletal muscle fibers (*arrows*) interspersed within the dense collagenous tissue, features consistent with teratoma.

Extraocular motor nerve tumors usually manifest with extraocular muscle palsy (5). Benign cranial nerve tumors include hamartoma (6, 7), lipoma (8), and schwannoma (5, 9). The most common primary extraocular nerve tumor is schwannoma (10, 11), which is frequently symptomatic (12). Despite their apparent predilection for sensory nerves, intracranial schwannomas also have been reported in pure motor and mixed sensorimotor cranial nerves, particularly in association with neurofibromatosis type 2. Reported, but much less common, tumors that affect the third nerve include lymphoma (13), glioblastoma (14), and meningioma (15). Cranial nerve granulomatous infiltration is relatively common (16) and should always be considered in the differential diagnosis. Although muscle-containing hamartomas and choristomas have been reported in the trigeminal (17, 18), facial and vestibulocochlear (19), and oculomotor nerves (20), the author could identify no prior reports of a teratoma arising from a cranial nerve.

Teratomas arise from totipotential cells and contain elements from all three germ cell layers including bone, cartilage, muscle, teeth, hair, fat, and sebum coexisting within the same lesion. Teratomas in multiple anatomic locations are reported but are principally encountered in the gonads, and account for only 0.5% to 2.0% of intracranial tumors. Most intracranial teratomas manifest in young children, and adult presentation is unusual. Central nervous system teratomas are extraaxial lesions originating from multipotential tissue rests and are identified primarily within the pineal and suprasellar third ventricular regions (21). Although this patient's mass was located within the oculomotor nerve, it is likely that the tumor initially arose from a multipotential tissue rest within the interpeduncular cistern in contiguity with the oculomotor nerve and was secondarily incorporated into the nerve.

The MR imaging differential diagnosis of an enhancing mass with high T1 and low T2 signal intensity (spin-echo sequence) includes aneurysm, teratoma, lipoma, dermoid tumor, exophytic brain stem glioma, hamartoma, meningioma, and schwannoma. Multiplanar imaging confirmation of a nonpedunculated extraaxial mass makes an exophytic glioma unlikely. The heterogeneous enhancement, high signal intensity on T1-weighted images, and location best support the diagnosis of a partially thrombosed basilar artery aneurysm or possibly a dermoid tumor. These features would not be characteristic of meningioma or schwannoma. Lipomas characteristically demonstrate high signal intensity on T1-weighted and low signal intensity on T2-weighted spin-echo images, and rarely demonstrate contrast enhancement. Mature teratomas contain fat; therefore, they are usually hyperintense on T1-weighted spin-echo images and demonstrate

suppression of high signal intensity on fat-suppressed T1-weighted images.

The CT features of this lesion allow one to narrow the differential diagnosis. Aneurysms are generally iso- to hyperattenuating on CT scans depending on the degree of thrombosis, but a hypoattenuating lesion is inconsistent with aneurysm at any stage of thrombosis. The CT imaging characteristics did not support schwannoma or meningioma either, as both are characteristically sharply delineated lesions isoattenuating to brain, with moderate to marked homogeneous contrast enhancement. Meningioma is particularly unlikely because of the lesion's location, lack of dural base, enhancement pattern, hypoattenuation (unenhanced meningiomas are usually 16–35 HU), and heterogeneity in the absence of calcification (8). Although schwannomas might exhibit hypoattenuation from cystic necrosis and enhancement characteristics varying from minimal heterogeneous to marked homogeneous (5), the marked hypoattenuation of this lesion would be an unlikely feature of schwannoma. At CT, lipomas are well-circumscribed, hypoattenuating lesions that typically do not enhance. Conversely, mature teratomas are well-marginated masses with heterogeneous hypoattenuating areas and sporadic calcification (9). Teratomas and dermoid tumors both show mixed attenuation and heterogeneous enhancement at CT, reflecting their varied composition.

Conclusion

A rare case of mature teratoma arising within the oculomotor nerve has been described. The radiologic appearance of a teratoma is determined by its diverse composition, and it might not be best demonstrated with only a single imaging modality. Characteristic imaging features of teratoma include fat signal intensity or attenuation, and heterogeneous enhancement. The lesion's high T1 signal intensity initially was attributed to thrombus within a basilar tip aneurysm, a more common lesion, because methemoglobin blood products are also bright on T1- weighted images. Hypoattenuation on CT scans confirmed that the high signal intensity within the mass on T1-weighted images was the result of fat rather than blood products. Comparison of fat-saturation T1-weighted images with unsaturated T1-weighted images, not available for this study, also would have confirmed the presence of fat by demonstrating loss of signal intensity in the previously hyperintense areas.

Acknowledgments

The author thanks Johnny B. Delashaw, MD, Peter J. Mitchell, MD, and Anthony N. D'Agostino, MD, for their assistance.

References

1. Biousse V, Newman N. **Third nerve palsies.** *Semin Neurol* 2000; 20:55–74
2. Bianchi-Marzoli S, Brancato R. **Third, fourth, and sixth cranial nerve palsies.** *Curr Opin Ophthalmol* 1997;8:45–51
3. Miller N. **Solitary oculomotor nerve palsy in childhood.** *Am J Ophthalmol* 1977;83:106–111
4. Rucker C. **The causes of paralysis of the third, fourth and sixth cranial nerves.** *Am J Ophthalmol* 1966;61:1293–1298
5. Okamoto S, Handa H, Yamashita J. **Neurinoma of the oculomotor nerve.** *Surg Neurol* 1985;4:275–278
6. Reid C, Fagan P, Turner J. **Cerebellopontine angle lipomatous hamartoma of nerve.** *Am J Otolaryngol* 1991;12:374–377
7. Zwick D, Livingston K, Clapp L, Kosnik E, Yates A. **Intracranial trigeminal nerve rhabdomyoma/choristoma in a child: a case report and discussion of possible histogenesis.** *Hum Pathol* 1989;20:390–392
8. Lee S, Rao K. **Primary tumors in adults.** In: Lee SH, Rao KCVG, eds, *Cranial Computed Tomography and MRI* 2nd ed. New York, NY: McGraw-Hill Book Co; 1987;303–350
9. Brandt-Zawadzki M, Kelly W. **Brain tumors.** In: Brandt-Zawadzki M, Norman D, eds. *Magnetic Resonance Imaging of the Central Nervous System.* New York, NY: Raven Press; 1987;151–185
10. Celli P, Ferrante L, Acqui M, Mastronardi L, Fortuna A, Palma L. **Neurinoma of the third, fourth, and sixth cranial nerves: a survey and report of a new fourth nerve case.** *Surg Neurol* 1992;38:216–224
11. Asaoka K, Sawamura Y, Murai H, Satoh M. **Schwannoma of the oculomotor nerve: a case report with consideration of the surgical treatment.** *Neurosurgery* 1999;45:630–633
12. Katoh M, Kawamoto T, Ohnishi K, Sawamura Y, Abe H. **Asymptomatic schwannoma of the oculomotor nerve: case report.** *J Clin Neurosci* 2000;7:458–460
13. Manabe Y, Kurokawa K, Kashihara K, Abe K. **Isolated oculomotor nerve palsy in lymphoma.** *Neurol Res* 2000;22:347–348
14. al-Yamany M, al-Shayji A, Bernstein M. **Isolated oculomotor nerve palsy: an unusual presentation of glioblastoma multiforme—case report and review of the literature.** *J Neurooncol* 1999;41:77–80
15. Hart A, Allibone J, Casey A, Thomas D. **Malignant meningioma of the oculomotor nerve without dural attachment: case report and review of the literature.** *J Neurosurg* 1998;88:1104–1106
16. Newman N, Slamovits T, Friedland S, Wilson W. **Neuro-ophthalmic manifestations of meningocerebral inflammation from the limited form of Wegener's granulomatosis.** *Am J Ophthalmol* 1995;120:613–621
17. Vajramani G, Devi I, Santosh V, et al. **Benign triton tumor of the trigeminal nerve.** *Childs Nerv Syst* 1999;15:140–144
18. Lena G, Dufour T, Gambarelli D, Chabrol B, Mancini J. **Choristoma of the intracranial maxillary nerve in a child: case report.** *J Neurosurg* 1994;81:788–791
19. Smith M, Thompson J, Thomas D, et al. **Choristomas of the seventh and eighth cranial nerves.** *AJNR Am J Neuroradiol* 1997;18:327–329
20. Frisen L, von Essen C, Roos A. **Surgically created fourth-third cranial nerve communication: temporary success in a child with bilateral third nerve hamartomas—case report.** *J Neurosurg* 1999;90:542–545
21. Salzman K, Rojiani A, Buatti J, et al. **Primary intracranial germ cell tumors: clinicopathologic review of 32 cases.** *Pediatr Pathol Lab Med* 1997;17:713–727